European Review for Medical and Pharmacological Sciences 2020; 24: 11496-11508

SGN nerve filaments develop synapses with IHCs earlier than with OHCs in C57BL/6 mouse inner ear

Z. HAN[1-4], J. DING[1-4], X. CHENG[1-4], Y.-L. HSIEH[1-4], C.-J. WANG[1-4], J.-Y. WANG[1-4], J.-M. YANG[1-4], N. CONG[1-4], F.-L. CHI[1-4]

[1]Department of Otology and Skull Base Surgery, Eye Ear Nose & Throat Hospital, Fudan University, Shanghai, China
[2]Department of Shanghai Auditory Medical Center, Shanghai, China
[3]NHC Key Laboratory of Hearing Medicine (Fudan University), Shanghai, China
[4]Fudan University, Shanghai, China

Zhao Han and Juan Ding contributed equally to the work

Abstract. – OBJECTIVE: To explore the connections between hair cells and spiral ganglion neurons (SGNs) during the development of the C57BL/6 mouse inner ear.

MATERIALS AND METHODS: The specimens of C57BL/6 mouse inner ear, from E15 (embryo day 15) to adult mouse, were collected; immunohistochemistry was employed to explore the frozen sections of specimens.

RESULTS: The development of cochlea starts sequentially from the basal turn to the apex turn. Morphological development of SGNs occurs mainly from E16 to P12 (postnatal day 12). Hair cells appear from E18 to P12, and inner hair cells (IHCs) develop earlier than outer hair cells (OHCs). The connections between hair cells and SGNs begin to develop during E18-P1, morphologically resemble mature synapses during P8-P12, and completely mature in adult mice.

CONCLUSIONS: The genesis of auditory ribbon synapse occurs from E18 to P1. Synchronized with the development of SGNs and hair cells, the functional filaments remain connected to hair cells, while the spare ones get disconnected from the surface of hair cells. Connections between SGN nerve filaments and IHCs occur earlier than those between SGN nerve filaments and OHCs.

Key Words:
TUJ-1, Peripherin, Neurofilament 200 kD, Inner ear, Cochlea, Spiral ganglion neurons, Afferent nerve, Efferent nerve.

Abbreviation

SGN: spiral ganglion neuron; IHCs: inner hair cells; OHCs: outer hair cells; ISSNHL: idiopathic sudden sensorineural hearing loss; IC/OC: inner cell/outer cell; TM: Tectorial membrane; AF: axis coelearis neurofilament; SL: spiral ligament; SC: supporting cell; SV: Stria vascularis; KO: Kolliker's organ; BM: basilar membrane; RM: Reissner's membrane; SV: spiral vessel. E1, 2, 3, etc.: embryonic day 1, 2, 3, and so on; E15: embryonic day 15, the day of embryo harvesting; P1, 2, 3, etc.: postnatal day 1, 2, 3, and so on; P22: postnatal day 22, the day of after weaning; SEM: Scanning electron microscopy; SD: Standard Deviation; SPSS: Statistical Product and Service Solutions.

Introduction

Hearing loss is a condition that disrupts human health. For example, idiopathic sudden sensorineural hearing loss (ISSNHL) occurs with a high incidence of 9.27/10,000 person-years[1]. Unlike in chick and zebrafish, sensorineural hearing loss is temporal and recovers by hair cell regeneration; it is usually permanent in adult mammals since the hair cells in their cochlea exhibit minimal spontaneous regeneration. Currently, otologic surgery and bionics, including cochlear implantation and hearing aid, are used to treat profound and extremely severe sensorineural hearing loss. Biological therapy, which is still under investigation in mammalian experiments, both *in vivo* and *in vitro*, includes molecular biology techniques, transgenic technology, and stem cell implantation for regeneration of hearing hair cells and the auditory nerve[2,3]. To find appropriate methods to reach our target, we need thoroughly to understand the developmental processes of the inner ear.

Corresponding Authors: Zhao Han, Ph.D; e-mail: sfhanzao@163.com
Ning Cong, MD; e-mail: congningent@126.com

The development of inner ear involves a lot of unknown details that are yet to be understood. A complete understanding of the details is required for developing steps for the regeneration of hair cells and treatment of hearing loss. There are many similarities and differences between the development and regeneration of hearing hair cells in mammals[4]. However, the details of the differences, consistency in the development, and regeneration of auditory nerve, and genesis of auditory ribbon synapse, remain unknown.

Wichmann et al[5] focused on the developmental steps of cochlea, including the mechanosensory contact of hearing hair cells and auditory nerve, and the functional mechanism of auditory ribbon synapses. Approximately 90-95% of spiral ganglion neurons (SGNs) are type I neurons projecting efferent and afferent filaments, whereas 5-10% are type II neurons[6,7]. As early as embryo day 16.5 (E16.5), type II SGNs are generated, according to the morphological characteristics of the auditory nerve[8], and immature inner hair cells (IHCs) begin to function[9]. However, mice achieve their hearing ability at postnatal day 12 (P12) or P14[10,11]. Although the development of auditory ribbon synapses occurs during *in utero* to postnatal day, all processes are not completely known in mammalian systems. As proven already, afferent synaptogenesis starts from postnatal day in mouse cochlea[12]. From the formation of SGNs and hair cells to the onset of hearing, hair cells, auditory nerves, and auditory ribbon synapses continuously keep adjusting themselves. Most studies on the development of cochlea *in vivo* have focused on either transgenic mouse or the working system of auditory ribbon synapse in normal mouse. However, research for exploring the exact details of the development of auditory nerve and ribbon synapse in mammalian cochlear development process is quite rare.

In this work, we focused on synaptogenesis between auditory nerves and hair cells during the development of normal mice. We explored the expression of certain proteins like TUJ-1[13], peripherin[7], neurofilament 200 kD[14], calbindin[15], NCS1 (frequenin)[16], myosin VIIa[17], neuroD1[17], islet1[17], and math1[18], which mark special structures of the inner ear during its development in the exact timeline from fetus to adulthood. These markers helped us to visualize the dynamic and morphologic development of special structures in the inner ear, as well as the key point timelines relevant for these structures.

Materials and Methods

Ethics Approval

All the procedures, performed in this research, were approved by the Institutional Animal Care and Animal Ethics Committee of Fudan University (Shanghai, China). Informed consent was obtained in accordance with the Declaration of Helsinki.

Tissue Samples

Cochleas were obtained from all the descendants of 60 mice (30 male and 30 female adult mice of C57BL/6 strain, supplied by the Department of Laboratory Animal Science, Medical College of Fudan University). Embryos were monitored as E1, 2, 3, etc. (embryonic day 1, 2, 3, and so on), and we harvested the embryo at E15. Similarly, we marked the postnatal days as P1, 2, 3, etc. After weaning, they were marked as P22.

By laparotomy, the uterus was harvested immediately after an overdose of anesthetics (ketamine and xylazine); the blastocyst was put in 4% paraformaldehyde solution at 4°C for 2 h, and the head was removed at E15. The head was soaked in 4% paraformaldehyde solution at 4°C for 2 h, followed by immersion in 15% sucrose solution at 4°C for 1 h, and then in OCT at 4°C for 2 h, before being sliced into frozen sections of 10 μm, in vertical position, using Leica CM3050S (Wetzlar, Germany). We stored the sections at –20°C, and the extra embryos at –80°C. At E16, we removed the cochlea out of the temporal bone, fixed it, and cut into frozen sections. Newly born mice were decapitated for cochlea, which were peeled off from the temporal bone in 4% paraformaldehyde solution at 4°C immediately and soaked in the solution for 4 h. The cochleas obtained were decalcified by 10% ethylenediaminetetraacetic acid (EDTA) messenger ribonucleic acid (mRNA) for 0-36 h, according to the different number of days. The adult mice were treated similarly. All the steps followed for cochlea, were also followed for the embryo.

Immunocytochemistry

Before being stained, the frozen sections were dried in a humidified box for 0.5-2 h at room temperature. At first, hematoxylin-eosin (HE) staining (using hematoxylin and eosin stain) was performed for overall morphology evaluation. The monoclonal antibodies used were: TUJ-1 (1:1000) (mouse monoclonal TUJ-1 to neuron

specific βIII tubulin (Abcam, Cambridge, MA, USA, Product No: ab14545), neurofilament 200 (1:400) (mouse monoclonal anti-neurofilament 200 clone NE14 Sigma-Aldrich, S. Louis, MO, USA, Product No: N5389), peripherin (rabbit polyclonal to peripherin, Abcam, Cambridge, MA, USA, Product No: ab4666), calbindin (1:500) (mouse monoclonal CL-300 to calbindin, Abcam, Cambridge, MA, USA, Product No: ab9481), myosin VIIa (1:400) (rabbit polyclonal to myosin VIIa, Abcam, Cambridge, MA, USA, Product No: ab3481), Islet1 (1:500) anti-Islet1 (rabbit polyclonal to islet1, Abcam, Cambridge, MA, USA, Product No: ab20670), neuroD1 (1:200) anti-neuroD1 (rabbit polyclonal to neuroD1, Abcam, Cambridge, MA, USA, Product No: ab16508), NCS1 (frequenin) (1:100) (anti-NCS1 chicken polyclonal to NCS1, Abcam, Cambridge, MA, USA, Product No: ab18060), and MATH1 (1:400) (anti-MATH1 rabbit polyclonal to MATH1, Abcam, Cambridge, MA, USA, Product No: ab13483). The secondary antibodies were from goat: rhodamine secondary antibody (1:200; goat polyclonal to chicken IgY H&L rhodamine, Abcam, Cambridge, MA, USA, Product No: ab6874), rhodamine secondary antibody (rhodamine-labeled affinity purified antibody to rabbit IgG (H+L) KPL Product No: 02-15-06, Delhi, India), and fluorescein secondary antibody (1:200; fluorescein-labeled affinity purified antibody to rabbit IgG (H+L), KPL, Product No: 03-15-06, Delhi, India).

Staining with monoclonal antibodies was performed as follows: the sections were placed in phosphate-buffered saline (PBS) for 10 min, 0.3% Triton for 1 h (not for membrane antigen), and 10% sera of goat for 20 min (5% fetal bovine serum (FBS) was used instead of goat sera when the secondary antibody was from goat), stained with the primary monoclonal antibody for 1 h at 37°C, and washed thrice with PBS for 5 min; the sections were stained with secondary antibodies for 1 h at 37°C in the dark, and washed thrice with PBS for 5 min. Finally, staining was performed with TOTO3 (1:5000) (nuclear counterstain and dead cell indicator) at 37°C for 30 min. The sections were mounted with 50% glycerinum and enamel and kept in the dark at 4°C until photographed. Steps for double or triple antibody staining are similar to those with one antibody; two or three antibodies were mixed with two or three secondary antibodies, separately, according to concentration ratio, before staining.

Image Acquisition and Analysis

Scanning electron microscopy (SEM) images were acquired with a Philips Quanta 200 SEM, and processed by Adobe Photoshop 7.0.1 (Adobe, San Jose, CA, USA) and 3D-DOCTOR for Windows. All confocal fluorescence images were taken with a Leica DMIRE2 Laser-scanning confocal microscope and Leica DFC300 FX (Wetzlar, Germany) image collecting system, and processed with a Leica QWin V3 image processing system. Since all the sections were cut from the top of the head perpendicular to the vertical axis (the thickness was 10 μm), we cut off sections parallel to the vertical axis with inner ear appearing. The 90º incisal margin of all the sections was positioned with respect to a fixed line under the microscope while collecting images.

Statistical Analysis

Statistical analysis was performed using Statistical Product and Service Solutions (SPSS) 22. 0 software (IBM, Armonk, NY, USA). Data were represented as mean ± SD (Standard Deviation). The *t*-test was used for analyzing measurement data. Differences between two groups were analyzed by Student's *t*-test. Comparison between multiple groups was performed using One-way ANOVA test followed by post-hoc test (Least Significant Difference). $p<0.05$ indicated a significant difference.

Results

Discrimination of SGNs, Afferent and Efferent Nerve Fibers of SGNs, IHCs, and OHCs

The cytoplasm and nucleus of SGNs were mainly labeled by neuroD1, islet1, and math1 separately, and the cell wall was stained by NCS1. The nerve fibers were stained by TUJ-1. The type I SGN projections were stained by neurofilament 200 kD, and the type II SGN projections were stained by peripherin. IHCs and OHCs were stained by calbindin from E19 to E22, and hair cells were stained by myosin VIIa before they were functionally mature.

Development of Cochlea Occurred in Sequence from Basal Turn to Apex Turn

The inner ear epithelium could be observed as early as E15 in the primary scala media. Development of cochlea occurred from the basal turn to apex turn as per the timeline of HE staining

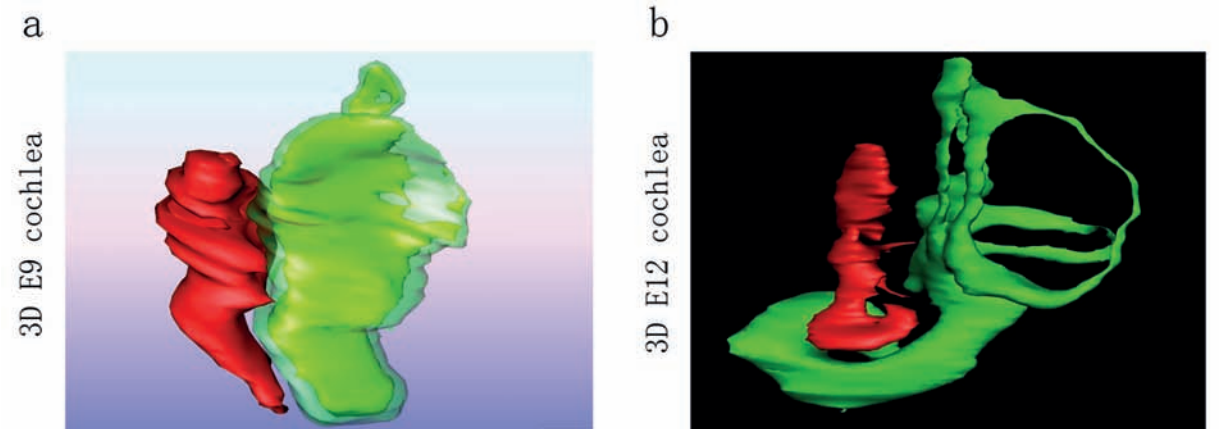

Figure 1. Cochlea develops from basal turn to apex turn (HE). **A,** 3D reconstructed structure of cochlea has a small part of basal turn at E9. **B,** and has the basal turn and half of the second turn at E12.

and 3D reconstruction (3D; Figures 1A, 1B). SGNs and hair cells could be recognized at E18 (SEM Figures 2A, 2B). From P2 to P4, the shape of OHCs was much more mature in the bottom than in the top turn; profiles of OHCs from the basal turn of cochlea and in vertical sections were more mature at P2 than those from the top turn of cochlea and in vertical sections (Figures 3A, 3B).

According to the development and spatiotemporal distribution of cochlea, the connection between SGNs and OHCs of basal turn was like a shallow goblet and the vertical part was distinct at P4 (Figures 4A, 4B, 4C); however, the connection with OHCs on the top turn was like a flat plate at the base of outer hair cells (Figures 4D, 4E, 4F), and the vertical part was not distinct. The differences between basal turn and top turn disappeared gradually until P7. Together, it implied that the development of top turn occurred 5 days later than that of basal turn[19].

Morphological Development of SGNs Mainly Occurred from E16 to P12

Nerve fibers projected by type II neurons accounted for 90-95% of total nerve fibers, while the remaining 5-10% were from type I neurons (Figure 5A, 5B, 5C). Type II nerve fibers reached the modiolus nerve fibers to form their connections (E18), which was 3 days earlier than the formation of connections between type I and modiolus nerve fibers (E21; Figure

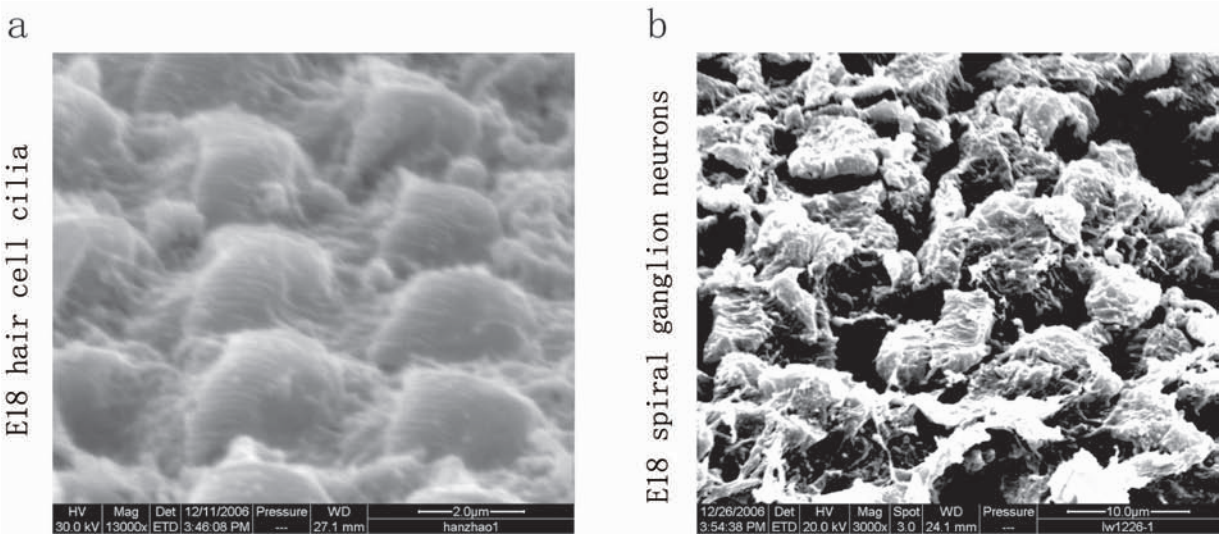

Figure 2. Profile of SGNs **(A)** and hair cells **(B)** under SEM at E18. SGNs could be recognized as connected to hair cells with fibrous joints, rather than synapses **(A)**; hair cells are connected to other cells, and the cilia are close to mature ones **(B)**.

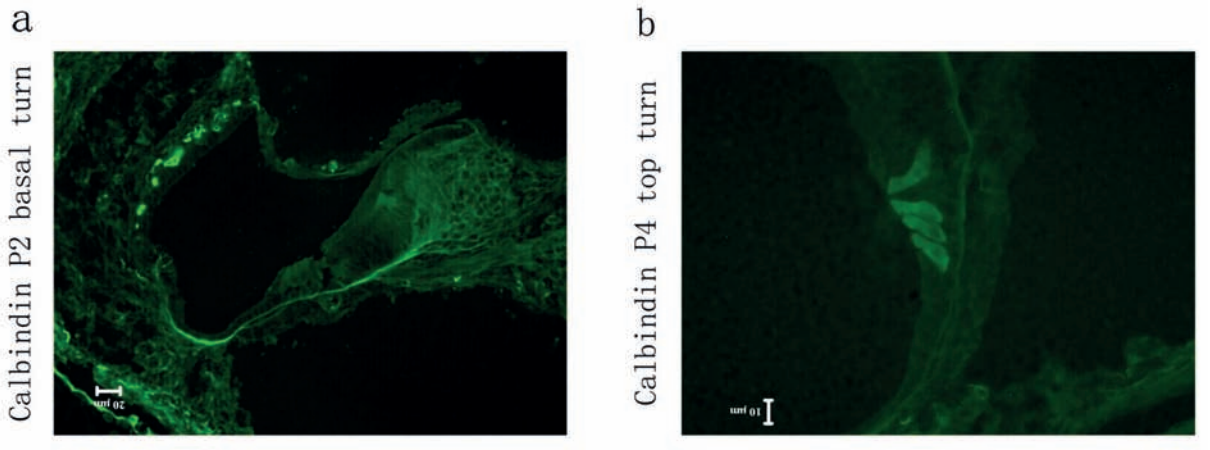

Figure 3. Shape of OHCs is much more matured in the bottom than in the top turn from P2 to P4 (stained by calbindin, green). The stained bottom of OHCs from the basal turn of cochlea is like a shallow goblet, and the vertical section of outer hair cells is strongly stained at P2 **(A)**, basal turn at P2. At P4, the stained bottom of OHCs from the top turn of cochlea is like a flat plate, whereas the vertical section of OHCs is stained weakly **(B)**, top turn, at P4.

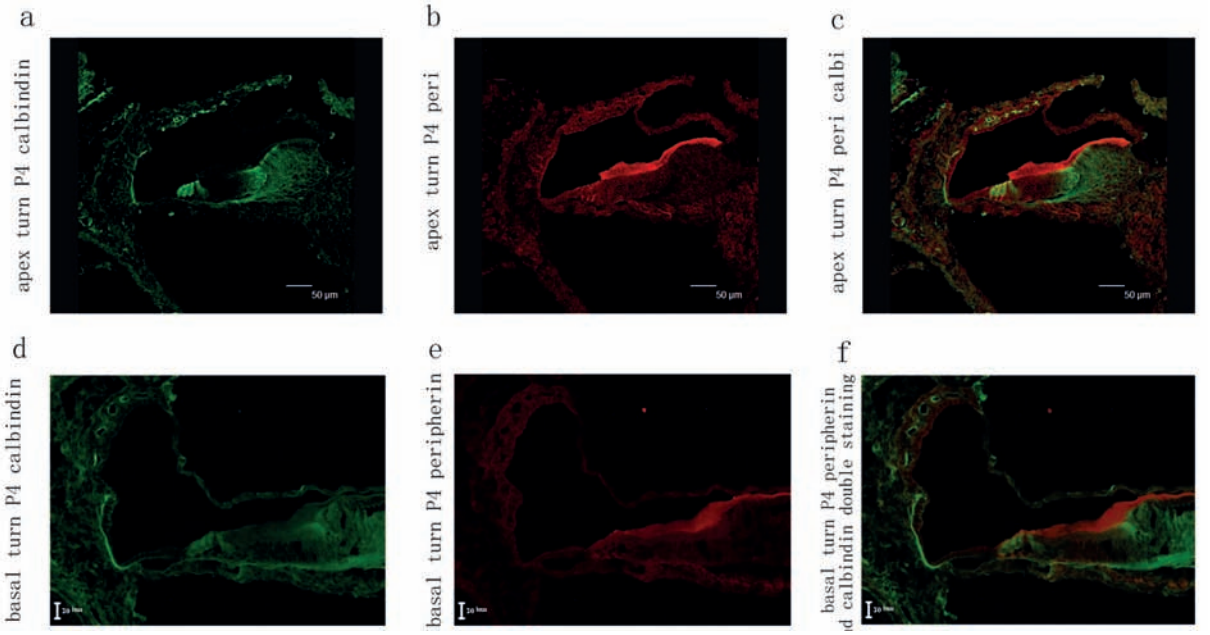

Figure 4. The connections between SGNs and OHCs of basal turn are more mature than those of the top turn (double labeling of red peripherin and green calbindin at P4). The connection with OHCs on the top turn is like a flat plate in the base of OHCs; however, the vertical part is not distinct (**A-C,**). The connection between SGNs and OHCs of basal turn is like a shallow goblet and the vertical part is distinct at P4 (**D-F,**).

6A, 6B). As early as E16, the SGNs were discriminated from other structures and their nuclear morphology matured from P8 to P12, as did their cytoplasmic morphology (or projecting nerve filaments; Figures 7, 8, 9).

Development of Hair Cells Could be Observed from E18 to P12: IHCs Occur Earlier Than OHCs

The cells programmed to become IHCs in the primordium of organum spirale were stained

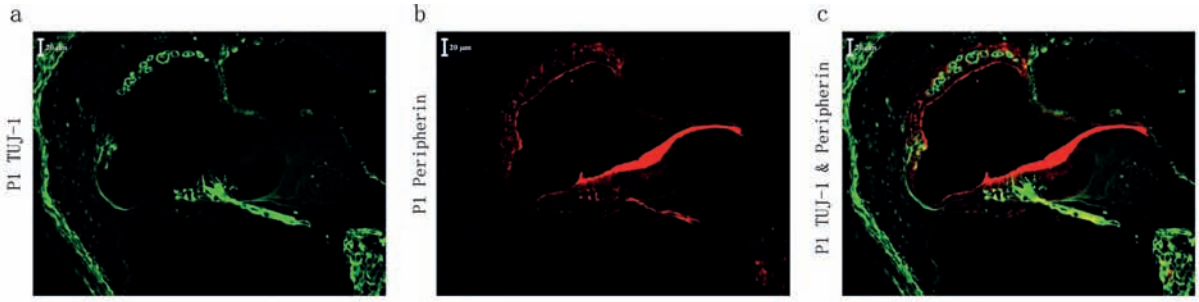

Figure 5. Nerve fibers projected by type II neurons are 90–95% of the total nerve fibers, while the remaining nerve fibers from type I neurons form 5–10%. Nerve filaments from type I and type II SGNs are different, as shown by peripherin **(A)**, TUJ-1 **(B)**, and double-labeling **(C)**.

by calbindin at E18 (Figure 10A), and the IHC profile was recognized just at E19 when their cytoplasm was stained. SEM images showed hair cells to be still connected to each other and the shape of cilia to be similar to those of mature ones at E18. OHCs could be observed from E18 and were distinct in shape at E21. The changes related to maturity, marked by myosin VIIa in hair cells, occurred from E21, rather than E18 (Figure 10B). Before P4, the profile of hair cells gradually resembled that of mature ones and began to function even when not mature enough in morphology at P12 (Figure 4A, 4B, 4C). During P1 to P7, IHCs and OHCs were active in producing proteins necessary for functional and morphological development, and production slowed down at P8 until P12, when the OHCs were not stained, and staining of IHCs by myosin VIIa just got weaker. The outline of hair cells was clear at P4, although they were not yet fully functional until the disappearance of myosin VIIa expression at P12.

The Connections Between Hair Cells and SGNs Continue to Develop During E18-P1, become Morphologically Close to Mature Synapses During P8-P12, and Completely Mature in Adult Mouse

As early as E15, nerve fibers projected by SGNs could be observed by the expression of TUJ-1, whereas type I and type II nerve fibers were found a day later on SGNs. At E18, hair cells and SGNs were connected by a few nerve filaments, although synapses were not yet formed. At E18, the formation of hair cells and their cilia, and SGNs and their filaments, was clearly observed under SEM; yet, fibrous joints, rather than synapses, could be found between hair cells and SGNs (Figure 11A, 11B, 11C). At E19, type II nerve filaments reached the top and bottom of

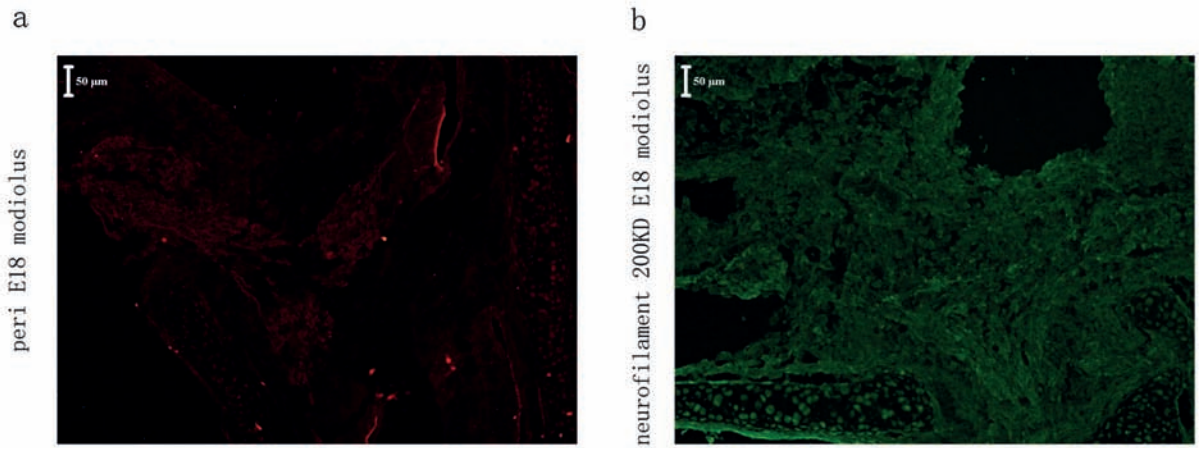

Figure 6. Development of type II nerve fibers occurs earlier than that of type I. Type II nerve fibers reach the modiolus nerve fibers for connection as early as at E18 (peripherin, **A,**); 3 days later, type I fibers reach at E21 (neurofilament 200 kD, **B,**).

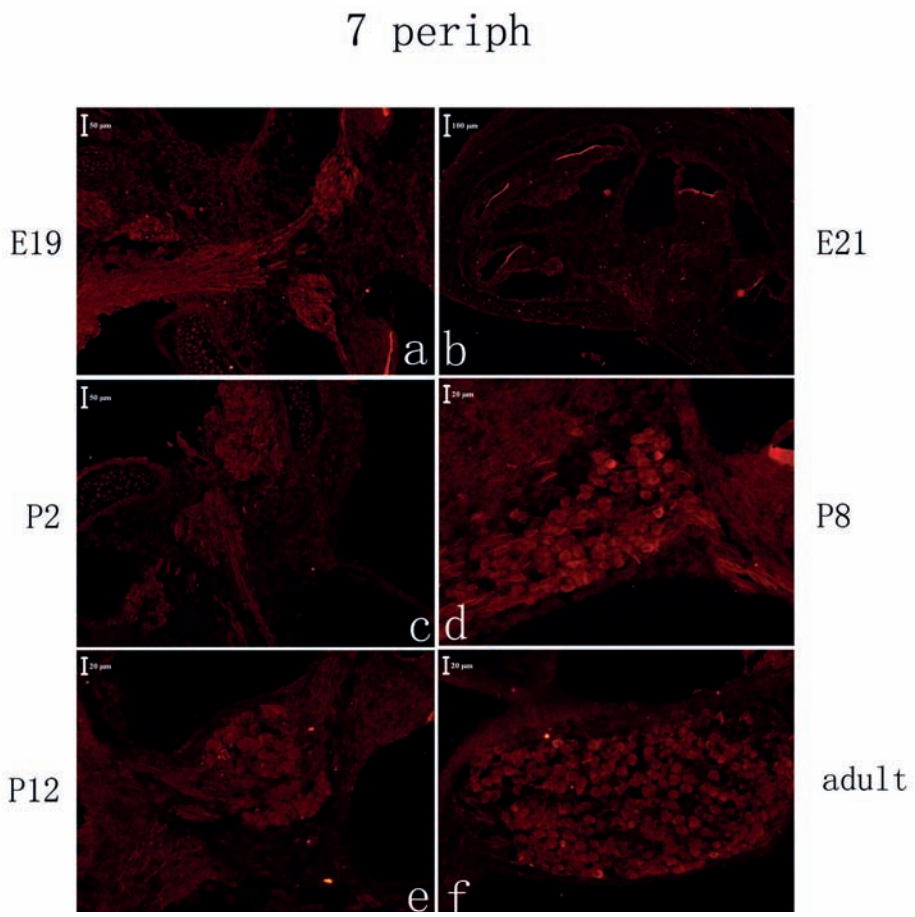

Figure 7. SGN morphology matures close to that of adults at P12 (stained by peripherin **(A)** E19; **(B)** E21; **(C)** P2; **(D)** P8; **(E)** P12; **(F)** adult); the nucleus matures morphologically from P8 to P12, as does the cytoplasm.

IHCs and OHCs and got stronger at E21; however, type I nerve filaments were just projected to hair cells, with no strong connections at E19, which became clear at E21 (Figure 12A, 12B, 12C). Until P5, the bottom of OHCs was connected by efferent filaments and circumvoluted IHCs (at E19, afferent filaments were clearly observed on IHCs). During P8 to P12, the hair cells were attached by nerve filaments and were morphologically similar to mature hair cells of the adult mice (Figure 13A, 13B, 13C and Figures 14, 15, 16).

Discussion

The Genesis of Auditory Ribbon Synapse Occurs During E18-P1

The development of spiral ganglion neurons is believed to have three distinct phases in mammalian cochlea: neurite growth, refinement, and retraction[20]. As reported in mice, auditory nerves may be divided into type I SGNs early at E10.5 and E12; they form independently and start projecting to otocyst from the hindbrain[21]. The efferent and afferent nerve fibers projecting to hair cells, labeled by ATP-gated ion channel P2X[1], were observed from E18[22]. Huang et al[20] found the immature type II and type I afferent filaments, labeled by peripherin and TMRD (tetramethylrhodamine-conjugated dextran), to innervate IHCs and the first row of OHCs at E18. These findings supported the fact that afferent and efferent nerve fibers from type I and type II spiral ganglion neurons reach OHCs and IHCs first at E18. Based on this knowledge, we started the present study from E15 and focused on the genesis of auditory ribbon synapses from E16. Our research not only supported the previous findings, but also revealed further information.

In the present study, type II nerve filaments reached the hearing epithelium at E18, and the rudiment of connection was formed at E21.

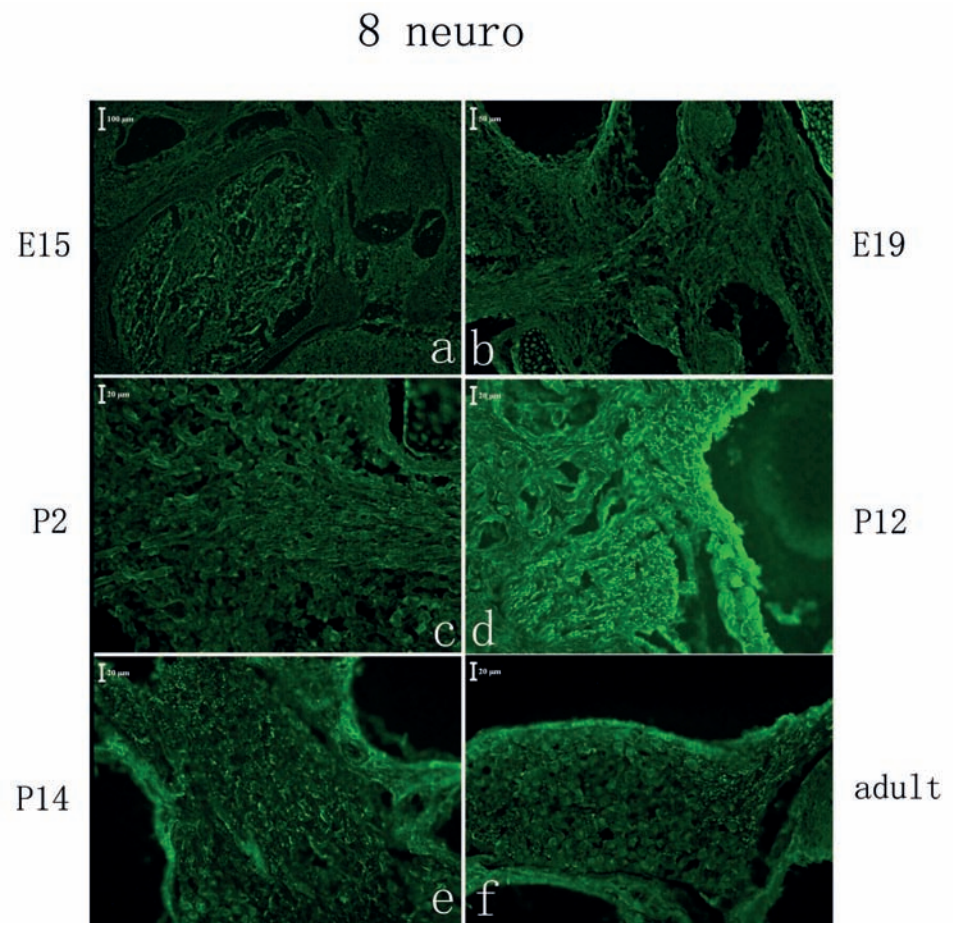

Figure 8. SGN morphology matures close to that of adults at P12 (stained by neurofilament 200 kD **(A)** E15; **(B)** E19; **(C)** P2; **(D)** P12; **(E)** P14; **(F)** adult); the nucleus matures morphologically from P8 to P12, as does the cytoplasm.

Type I filaments arrived at cochlear duct coils at E19 and built the connection with hair cells at P1. Consequently, we observed that the connections between hair cells and SGNs are formed from E18 to P1.

Synchronizing with the Development of SGNs and Hair Cells, the Functional Filaments Remain Connected to Hair Cells, while the Spare Ones Get Disconnected from the Surface of Hair Cells

Both IHCs and OHCs were projected by type I neurons, the processes being retracted from OHCs to form synapses with IHCs, and processes from type II SGNs retracted from IHCs to form synapses with OHCs[23-25]. Considering the binding site between fiber bundle and hair cells, the filaments stained by the attachment of peripherin to the bottom of IHCs should be afferent filaments, as verified by other reports[26]. At E19, 4-5 filaments stretched to the bottom of IHCs, and only one thin filament was left at P1. At E16, the intensity of afferent filaments was almost the same; however, till P10, only a few filaments were still strongly connected to IHCs. At P3, there were visible connections from efferent nerve fibers to hair cells, and at P5, the IHCs were apparently circumvoluted by efferent nerve filaments; only a few SGNs next to the Habenula tube and modiolus were type I neurons. We can extend our study to show that during the changes in connection and disconnection of filaments, the former was getting strong and clear, while the spare nerve fibers were retracting, so that the functional fibers became continuous and thinner.

However, a there is still a question about what makes the spare filaments contract. The answer may be in the gene regulation of type II fibers stained by peripherin[22]. As we know, environ-

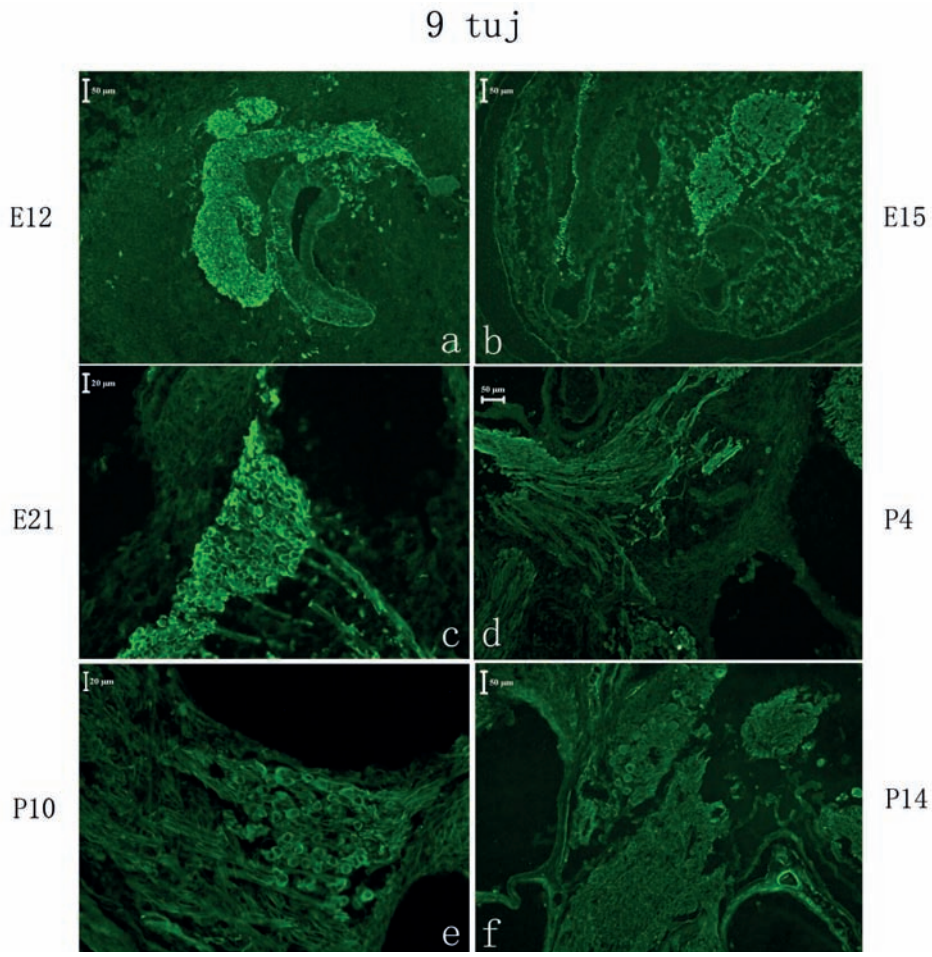

Figure 9. SGN morphology matures close to that of adults at P12 (stained by TUJ-1 **(A)** E12; **(B)** E15; **(C)** E21; **(D)** P4; **(E)** P10; **(F)** P14). The nucleus matures morphologically from P8 to P12, as does the cytoplasm.

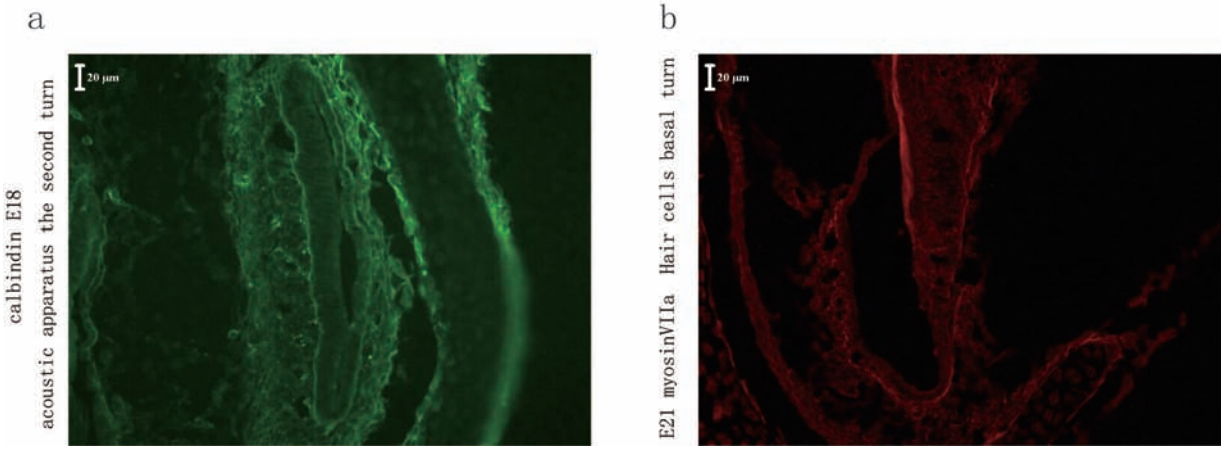

Figure 10. IHC is dormant during E18 to E21 of its initial observation. IHCs can be found at E18 (calbindin is green) **(A)**. The cells, becoming IHCs in the primordium of organum spirale, were stained by calbindin at E18. Hair cells mature from E21 (myosin VIIa is red) **(B)**. The maturation changes of hair cells from E21 are marked by myosin VIIa in the basal turn.

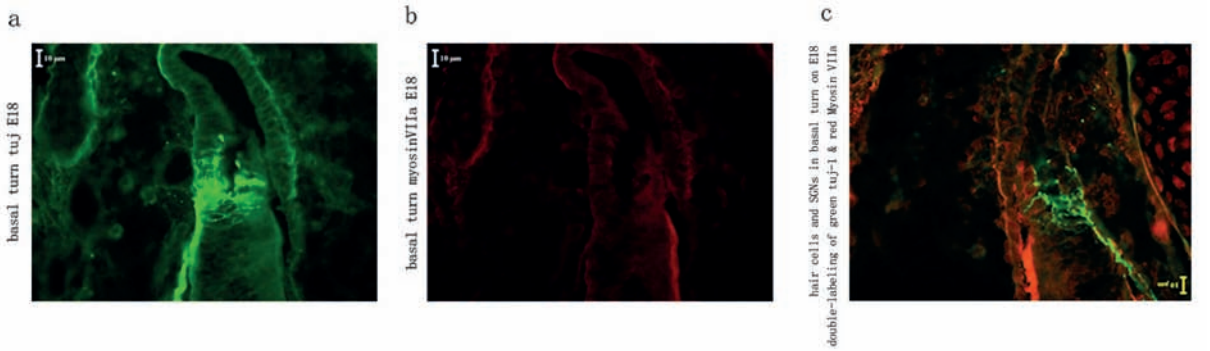

Figure 11. Hair cells and SGNs are connected immaturely by filaments at E18 (TUJ-1 is green, myosin VIIa is red). The fibrous joint (not synapses) could be found between hair cells and SGNs at E18. The basal turn stained by TUJ-1 **(A)**, myosin VIIa **(B)**, and double-labeling of TUJ-1 and myosin VIIa **(C)**.

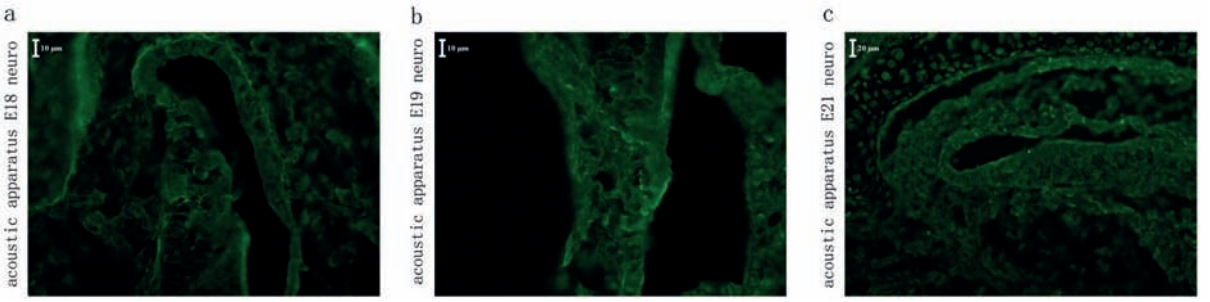

Figure 12. The connection between type I nerve filament and hair cells in the acoustic apparatus becomes clear at E21 (neurofilament 200 kD is green). Figures **A-C,** show images stained by neurofilament 200 kD in the acoustic apparatus at E18, E19, and E21, respectively. Type I nerve filament is just projected to hair cells and the connections are not obvious at E18; it does not get strong or clear at E19 and is clearly observed at E21.

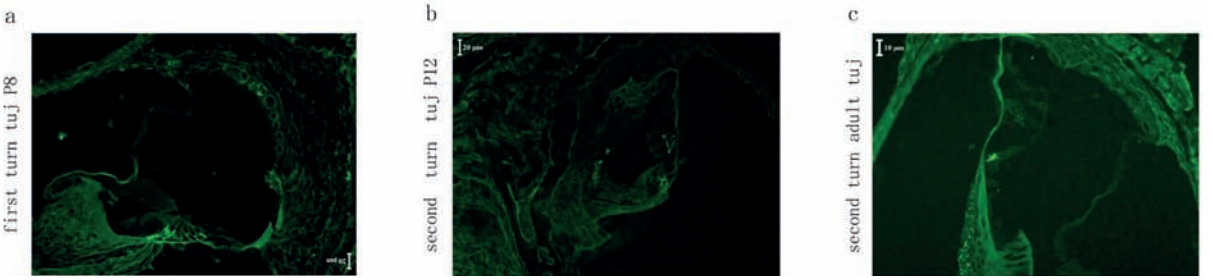

Figure 13. The connection between SGN nerve filament and hair cells is morphologically similar to mature synapse at P12. Labeling of TUJ-1 at P8 **(A)**; labeling of TUJ-1 at P12 **(B)**. During P8 to P12, the hair cells are attached by nerve filaments and were morphologically similar to mature synapse of adults. Labeling of TUJ-1 in adults **(C)**.

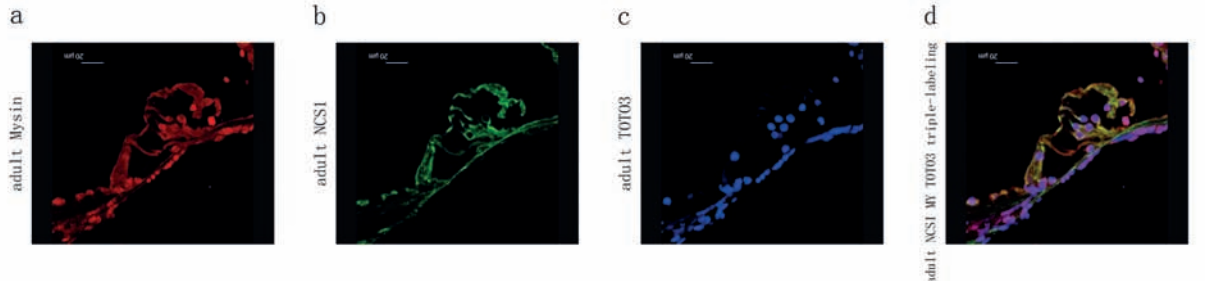

Figure 14. Triple-labeling of myosin VIIa, NCS1, and TOTO3. Labeling of myosin VIIa in adult, red **(A)**; of NCS1 in adult, green **(B)**; of TOTO3 in adult, blue **(C)**; triple-labeling of myosin VIIa, NCS1, and TOTO3 **(D)**.

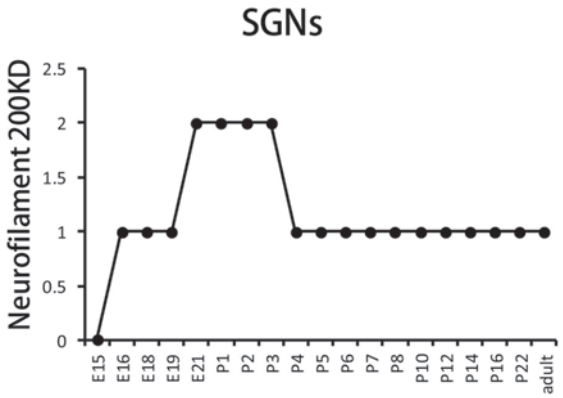

Figure 15. Timetable of the expression of neurofilament.

mental stimulation affects the formation of efferent neurites[27], and the efferent connections with hair cells modulate the mechanoreceptors of hair cell and the brain[28]. The formation and remodeling of afferent synapses may be regulated by the maturation of efferent synapses[29]. We can assume that environmental stimulation contributes to the formation of auditory ribbon synapses by the selection of filaments.

Development of Connections Between SGN Nerve Filaments and IHCs Occurs Earlier Than That Between SGN Nerve Filaments and OHCs

TMRD and neurofilament 200 kD were proven to label type I nerve filaments[14,20]; there is only one row of IHCs and three rows of OHCs in the Corti's organ. Staining of TMRD could be observed from E18, when IHCs and the first row of OHCs were stained, excluding the second and third rows[20]. Thus, we concluded that at E18, connections between type I nerve filaments and IHCs, but not between type I nerve filaments and OHCs, are formed. As reported, at the beginning[23-25], the nerve filaments projected by SGNs run disorderly and unsystematically to hair cells. In our study, the connections between SGNs and hair cells were stained by neurofilament 200 kD from E21, which specially marked both connections of IHCs and all three rows of OHCs. We, therefore, suggested that the connections between type I nerve filaments and IHCs are formed before E21, and that between type I nerve filaments and OHCs are newly formed at E21.

In the present study, the connections between type II nerve filaments and hair cells were marked by peripherin at E18, and type II filaments connected to IHCs and to all three rows of OHCs. From P3 to P6, the type I nerve filaments were connected to IHCs, and no type II nerve filaments were left, whereas type II was connected to OHCs with just a few residual type I nerve filaments left[20]. We, therefore, conclude that the connections between type II nerve filaments and IHCs are formed before E18, while those between type II nerve filaments and OHCs are newly formed at E18. Thus, taken together, the connections between SGN nerve filaments and IHCs are formed by E18, while those between SGN nerve filaments and all three rows of OHCs are not formed until E21.

Qualitatively, the adjusted connections of type I nerve filaments and IHCs, and the adjusted connections of type II nerve filaments and OHCs, mainly developed from P6, whereas the connections of type I nerve filaments with OHCs, and those of type II nerve filaments with IHCs were refined due to the contraction of spare filaments.

Conclusions

The genesis of auditory ribbon synapse occurs during the period of E18 to P1. Synchronizing with the development of SGNs and hair cells, the functional filaments remain connected to hair cells, while the spare ones get disconnected. Development of the connections between SGN nerve filaments and IHCs occurred earlier than that between SGN nerve filaments and OHCs.

Our results provide a direction to promote research on the function of hair cell regeneration.

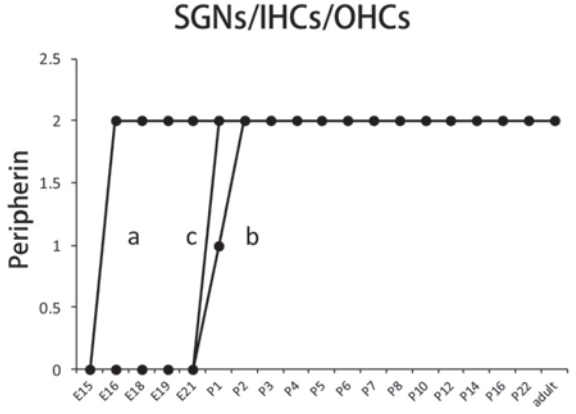

Figure 16. Timetable of the expression of peripherin, indicating spiral ganglion neurons (SGNs; **A,**) and inner hair cells/outer hair cells (IHCs, **B,** OHCs, **C,** respectively).

Further, our finding that the synaptic contact between regenerative hair cells and new nerve endings is first extensive and then modified according to function has certain implications for the clinical treatment of sudden deafness. In the process of treatment, while retaining hair cells, drugs that promote nerve growth should be used. At the same time, patients should be exposed to appropriate sound stimulation, which is helpful for the re-innervation and modification of hair cells and nerves.

Conflict of Interest

The Authors declare that they have no conflict of interests.

Funding acknowledgements

The work was supported by NSFC 81371093, 18ZR1406100 to Zhao Han. The National Key Research and Development Program of China (No. 2016YFC0905200) to Fanglu Chi.

References

1) Chiu CC, Lee KJ, Weng SF, Yang YM, Lin YS. Gallstone is correlated with an increased risk of idiopathic sudden sensorineural hearing loss: a retrospective cohort study. BMJ Open 2015; 5: e9018.
2) Santaolalla F, Salvador C, Martinez A, Sanchez JM, Del RA. Inner ear hair cell regeneration: A look from the past to the future. Neural Regen Res 2013; 8: 2284-2289.
3) Han Z, Yang JM, Chi FL, Cong N, Huang YB, Gao Z, Li W. Survival and fate of transplanted embryonic neural stem cells by Atoh1 gene transfer in guinea pigs cochlea. Neuroreport 2010; 21: 490-496.
4) Atkinson PJ, Huarcaya NE, Sayyid ZN, Cheng AG. Sensory hair cell development and regeneration: similarities and differences. Development 2015; 142: 1561-1571.
5) Wichmann C, Moser T. Relating structure and function of inner hair cell ribbon synapses. Cell Tissue Res 2015; 361: 95-114.
6) Simmons DD, Liberman MC. Afferent innervation of outer hair cells in adult cats: II. Electron microscopic analysis of fibers labeled with horseradish peroxidase. J Comp Neurol 1988; 270: 145-154.
7) Hafidi A, Despres G, Romand R. Ontogenesis of type II spiral ganglion neurons during development: peripherin immunohistochemistry. Int J Dev Neurosci 1993; 11: 507-512.
8) Koundakjian EJ, Appler JL, Goodrich LV. Auditory neurons make stereotyped wiring decisions before maturation of their targets. J Neurosci 2007; 27: 14078-14088.
9) Johnson SL, Marcotti W, Kros CJ. Increase in efficiency and reduction in Ca2+ dependence of exocytosis during development of mouse inner hair cells. J Physiol 2005; 563: 177-191.
10) Wong AB, Rutherford MA, Gabrielaitis M, Pangrsic T, Gottfert F, Frank T, Michanski S, Hell S, Wolf F, Wichmann C, Moser T. Developmental refinement of hair cell synapses tightens the coupling of Ca2+ influx to exocytosis. EMBO J 2014; 33: 247-264.
11) Mikaelian D, Alford BR, Ruben RJ. Cochlear potentials and 8 nerve action potentials in normal and genetically deaf mice. Ann Otol Rhinol Laryngol 1965; 74: 146-157.
12) Sobkowicz HM, Rose JE, Scott GE, Slapnick SM. Ribbon synapses in the developing intact and cultured organ of Corti in the mouse. J Neurosci 1982; 2: 942-957.
13) Fanarraga ML, Avila J, Zabala JC. Expression of unphosphorylated class III beta-tubulin isotype in neuroepithelial cells demonstrates neuroblast commitment and differentiation. Eur J Neurosci 1999; 11: 517-527.
14) Despres G, Leger GP, Dahl D, Romand R. Distribution of cytoskeletal proteins (neurofilaments, peripherin and MAP-tau) in the cochlea of the human fetus. Acta Otolaryngol 1994; 114: 377-381.
15) Liu W, Davis RL. Calretinin and calbindin distribution patterns specify subpopulations of type I and type II spiral ganglion neurons in postnatal murine cochlea. J Comp Neurol 2014; 522: 2299-2318.
16) Hamasaki-Katagiri N, Molchanova T, Takeda K, Ames JB. Fission yeast homolog of neuronal calcium sensor-1 (Ncs1p) regulates sporulation and confers calcium tolerance. J Biol Chem 2004; 279: 12744-12754.
17) Nguyen K, Hall AL, Jones JM. Expression of myosin VIIA in the developing chick inner ear neurons. Gene Expr Patterns 2015; 19: 36-44.
18) Bermingham NA, Hassan BA, Price SD, Vollrath MA, Ben-Arie N, Eatock RA, Bellen HJ, Lysakowski A, Zoghbi HY. Math1: an essential gene for the generation of inner ear hair cells. Science 1999; 284: 1837-1841.
19) Chi FL, Han Z, Dai PD, Huang YB, Cong N, Li W. Three-dimensional reconstruction of C57BL/6 mouse inner ear during development. ORL J Otorhinolaryngol Relat Spec 2009; 71: 334-341.
20) Huang LC, Thorne PR, Housley GD, Montgomery JM. Spatiotemporal definition of neurite outgrowth, refinement and retraction in the developing mouse cochlea. Development 2007; 134: 2925-2933.
21) Fritzsch B, Nichols DH. DiI reveals a prenatal arrival of efferents at the differentiating otocyst of mice. Hear Res 1993; 65: 51-60.
22) Barclay M, Julien JP, Ryan AF, Housley GD. Type III intermediate filament peripherin inhibits neuritogenesis in type II spiral ganglion neurons in vitro. Neurosci Lett 2010; 478: 51-55.
23) Coate TM, Spita NA, Zhang KD, Isgrig KT, Kelley MW. Neuropilin-2/Semaphorin-3F-mediated repulsion promotes inner hair cell innervation by spi-

ral ganglion neurons. eLife 2015; 4. doi: 10.7554/eLife.07830.

24) Huang LC, Barclay M, Lee K, Peter S, Housley GD, Thorne PR, Montgomery JM. Synaptic profiles during neurite extension, refinement and retraction in the developing cochlea. Neural Dev 2012; 7: 38.

25) Barclay M, Ryan AF, Housley GD. Type I vs type II spiral ganglion neurons exhibit differential survival and neuritogenesis during cochlear development. Neural Dev 2011; 6: 33.

26) Fryatt AG, Vial C, Mulheran M, Gunthorpe MJ, Grubb BD. Voltage-gated sodium channel expression in rat spiral ganglion neurons. Mol Cell Neurosci 2009; 42: 399-407.

27) Delano PH, Elgueda D, Ramirez F, Robles L, Maldonado PE. A visual cue modulates the firing rate and latency of auditory-cortex neurons in the chinchilla. J Physiol Paris 2010; 104: 190-196.

28) Rabbitt RD, Brownell WE. Efferent modulation of hair cell function. Curr Opin Otolaryngol Head Neck Surg 2011; 19: 376-381.

29) Simmons DD. Development of the inner ear efferent system across vertebrate species. J Neurobiol 2002; 53: 228-250.